

Experimental investigation on the shimmy phenomenon

D. De Falco ^{*}, G. Di Massa [#], S. Pagano [†]

^{*} Dipartimento di Ingegneria
Aerospaziale e Meccanica
Seconda Università di Napoli
Via Roma 29, 80100 Aversa, Italy
e-mail: domenico.defalco@gmail.com

[#] Dipartimento di Meccanica ed Energetica
Università di Napoli Federico II
Via Claudio 21, 80125 Napoli, Italy
e-mail: gdimassa@unina.it

[†] Dipartimento di Meccanica ed Energetica
Università di Napoli Federico II
Via Claudio 21, 80125 Napoli, Italy
e-mail: pagano@unina.it

ABSTRACT

The dynamic behavior of motorcycles, in terms of out of plane vibration modes, is strongly influenced by relative oscillations that can arise between the front and rear frames around the steering axis. When idealizing behavior for a rear frame mass which is very large compared with the front frame, the shimmy phenomenon takes place.

This paper presents a basic experimental investigation of the shimmy phenomenon of a scooter front assembly whose wheel is supported by a constant velocity translating belt. The tests were performed using different sets of parameters that influence the dynamic behavior of the system. For every operational condition, the damping needed to stabilize the system was found by properly adjusting the anti-shimmy damper; the investigation results are mainly reported in terms of damping-speed diagrams.

Keywords: castor, shimmy, stability.

1 INTRODUCTION

The term “castor” is used to define any swivel wheel whose contact patch area with the ground lies behind the intersection of the steering axis with the ground. The study of castor shimmy oscillations regards a number of applications, even if there are some differences. For two-wheel vehicles, these oscillations are very dangerous since they occur with a frequency that cannot be controlled by the rider; furthermore, they lead to an increase in rolling resistance, tire wear and fatigue stress in the castor components.

The first scientific papers on the shimmy phenomenon were published about 80 years ago, but many details of the phenomenon mechanism have not yet been fully understood since it depends on a great number of factors such as overall vehicle dynamics, geometric/inertial castor characteristics, compliance and damping of the castor components, backlashes and tire characteristics [1], [2], [3], [4], [5].

In [5] a three-dimensional castor dynamics model that can be used to study the system stability and evaluate the damping needed to stabilize the castor for different operational conditions was developed.

To study the castor dynamics experimentally, a test rig was set up and the first results are reported in this paper.

2 THE TEST RIG

The test rig adopted for the investigation consists (Fig. 1) of a castor, derived from a commercial scooter front assembly, joined to a rigid steel frame by means of a support that allows the castor to vertically translate and rotate around its steering axis. Furthermore, the support (Fig.2) allows the rake angle to be adjusted using a screw adjustment and a vertical load can be added to the castor, by means of masses joined to the castor with a wire rope and a system of pulleys. Castor rotation is counteracted by a 18 position (click) adjustable steering damper and two replaceable helical springs that provide rotational stiffness.

The castor wheel rolls on a flat track, made up of a composite material belt rolling up on two rolls and driven by an electric motor [6].

The test rig allows to set:

- a) belt speed;
- b) rake angle;
- c) vertical load;
- d) fork suspension extension;
- e) steer damping;
- f) rotational stiffness.

Since the force exerted by the steering damper depends almost linearly on the steer rotating speed, the damping value for each of the first 9 damper positions (clicks) was estimated. Starting from the damper characteristic curves and taking into account the damper arm with respect to the steering axis (124mm), the rotational damping coefficients σ , associated with each damper click, are:

click	0	1	2	3	4	5	6	7	8
σ [Nms/rad]	0.615	0.661	0.723	0.938	1.29	1.44	1.75	2.20	2.61

Table I – Viscous damping coefficients

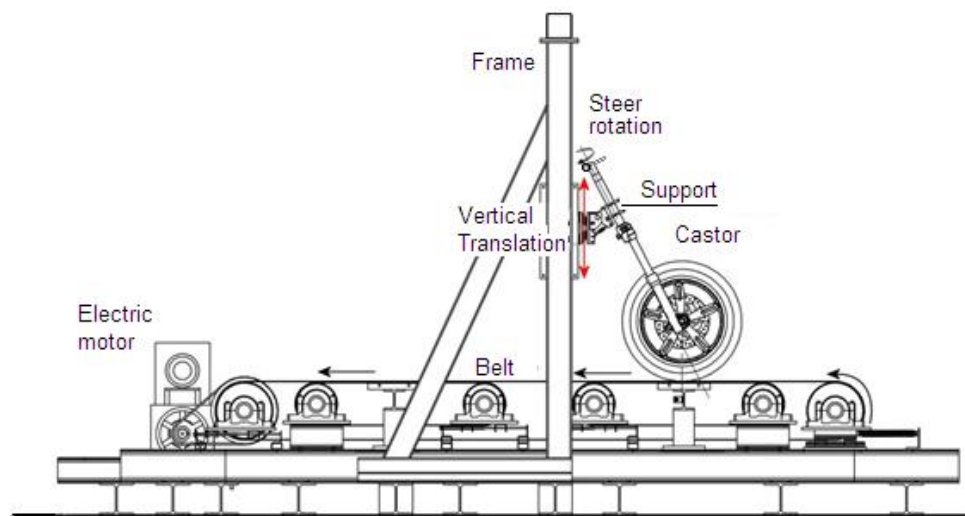


Figure 1 – Test rig scheme

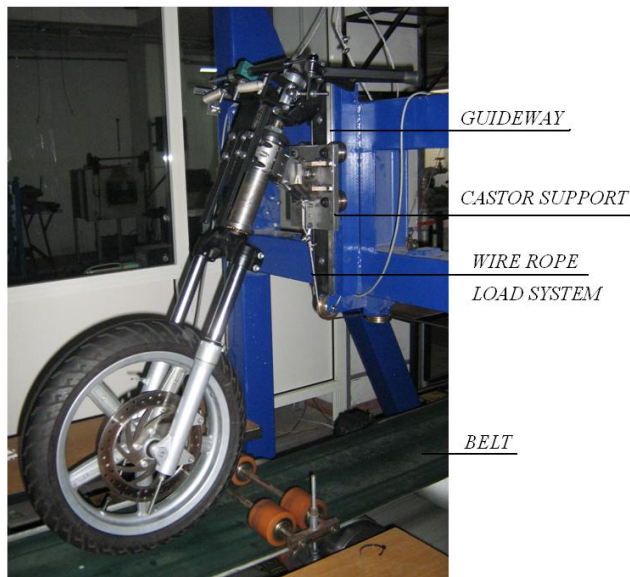


Figure 2 a - Castor on the belt rig

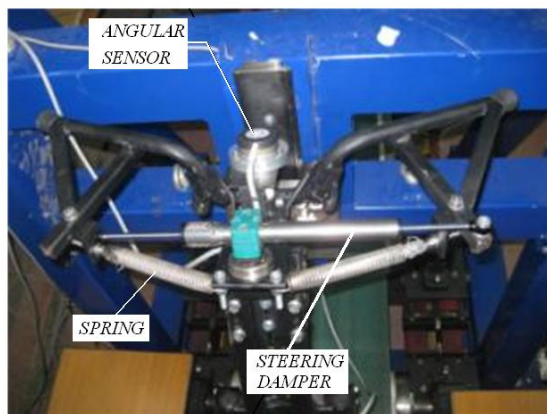


Figure 2b – Castor handlebar

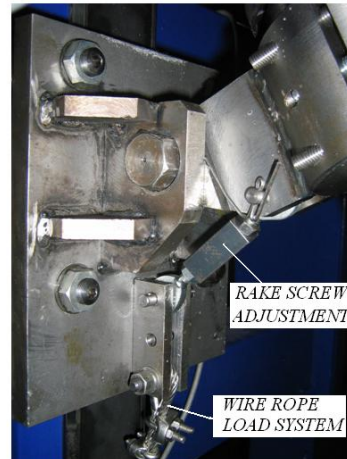


Figure 2c – Castor support

Figure 2a shows a photo of the castor on the belt rig, Figure 2b shows a view of the handlebar equipped with the damper and the angular sensor and Figure 2c shows a detail of the castor support with the rake angle adjustment screw.

Considering the fork castor as a planar frame, its lateral stiffness depends on its cubed length and it is therefore strongly influenced by the fork extension. In turn, fork extension depends on the vertical load acting on the castor itself but it is not possible to establish a relationship between the vertical load and lateral stiffness with certainty because a unique extension value does not correspond to a given vertical load value due to the force friction that arises between the suspension sliding surfaces.

Figure 3 shows the load-travel diagram for one telescopic suspension in vertical axis configuration; due to the greater friction force, the difference between the compression and the extension branches is greater for inclined suspension.

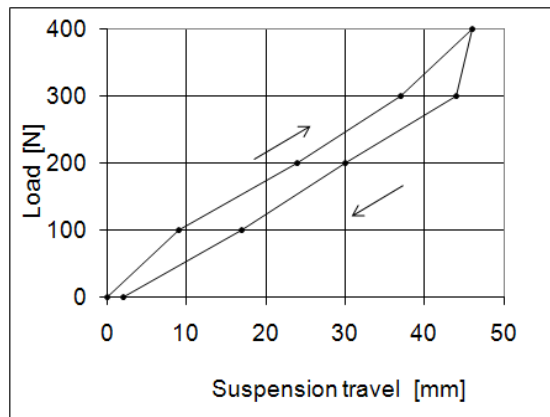


Figure 3 - Suspension load-travel diagram

To investigate the vertical load effect, independently of the lateral stiffness variation, the suspension springs were replaced by rigid spacers and locked in a given extension. Figure 4 shows the original suspension (a), together with the modified one in the maximum (b) and minimum (c) extension configurations.

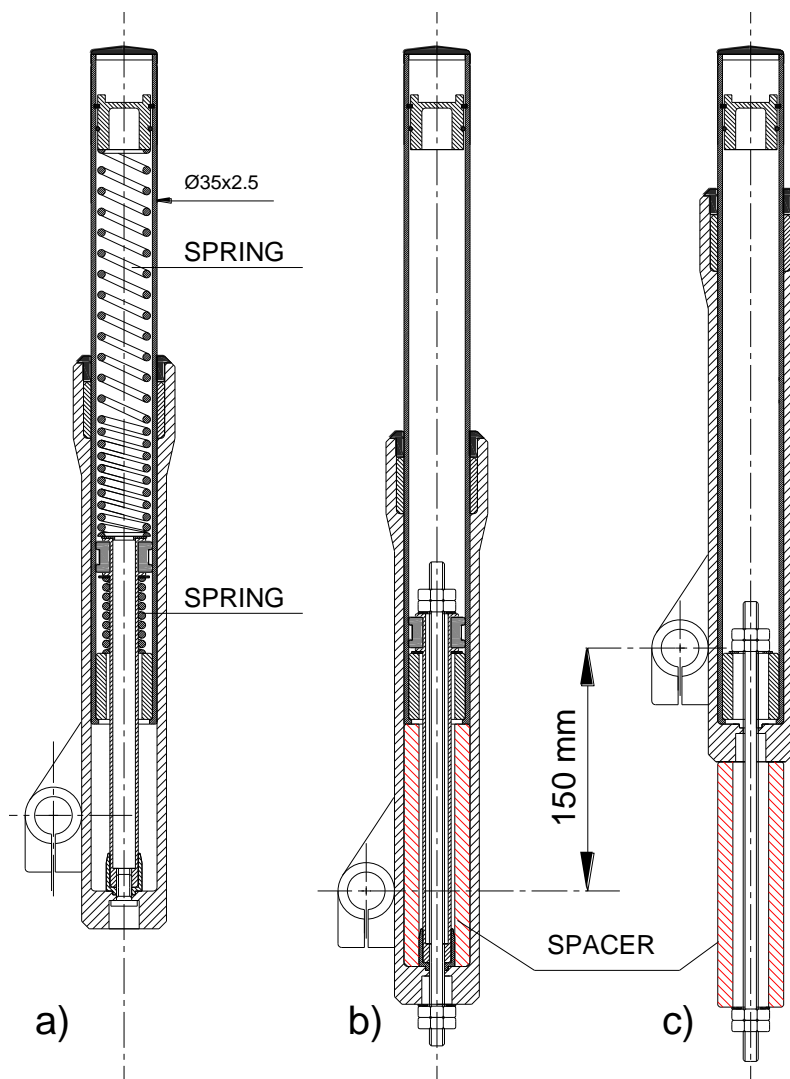


Figure 4 - Suspension modification:
a) original configuration; b) maximum extension; c) minimum extension.

The spacers are fitted outside the suspension in the minimum extension configuration (Fig. 4c, 5) so that the moment of inertia of the castor, with respect to the steering axis, does not change with the fork configuration; the moment of inertia value was identified as 0.37kgm^2 by means of a free oscillation test.

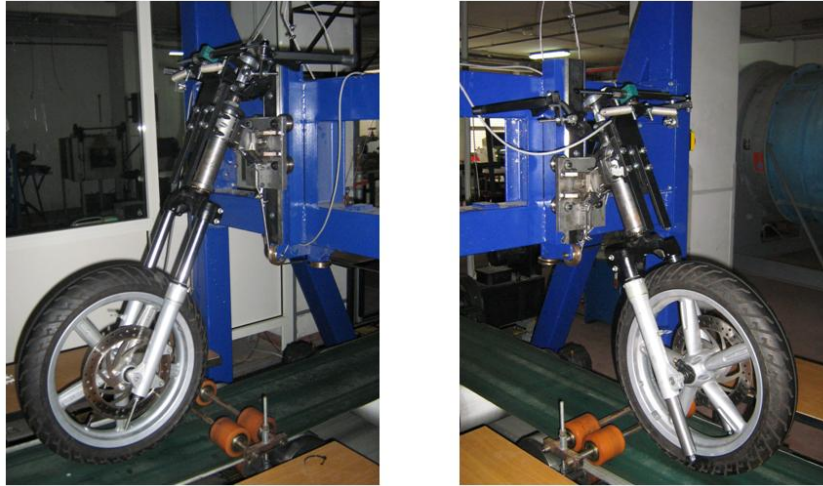


Figure 5 - Maximum and minimum fork extension

The fork length difference, between the two extreme configurations, is equal to 150 mm and implies significant stiffness differences as shown in Table II (where the results of static load tests are reported) .

	Lateral stiffness [N/m]	Torsional stiffness [Nm/rad]
Max extension	150000	5000
Min extension	250000	8000

Table II - Fork stiffness

The tire used for the tests (100/80 – 16” 50P) was characterized with the *rotating disk tire test machine* [4] at the University of Padua. The wheel characteristics are reported in Table III:

TIRE 100/80 - 16" 50P	
Type	Tubeless
Cornering stiffness coefficient - $F_z=721\text{ N}$	13,43 1/rad
Cornering stiffness coefficient - $F_z=972\text{ N}$	12,34 1/rad
Cornering stiffness coefficient - $F_z=1289\text{ N}$	10,45 1/rad
Relaxation length	208 mm
Tire-wheel weight	8,85 kg
Tire-wheel polar moment of inertia	$0,324\text{ kgm}^2$
Tire-wheel diametral moment of inertia	$0,201\text{ kgm}^2$

Table III - Wheel characteristics

3 EXPERIMENTAL RESULTS

It is known that a castor can exhibit stable behavior or shimmy oscillations when the forward speed is varied. For the tested castor, the steering angle sensor signal was detected for different values of the belt speed and the corresponding FFTs, reported as a waterfall in Figure 6, show that:

- for low speed values, the system oscillates with small amplitude and with a frequency of about 5 Hz;
- for a speed of 25km/h, the shimmy oscillations assume maximum amplitude with a frequency of about 5.4 Hz;
- for a further increase of the speed, the shimmy amplitude decreases while the frequency continues to grow almost linearly with the speed (7Hz at 65km/h);
- for a speed of 70 km/h, the shimmy oscillation disappears:
- the straight line reported in the diagram represents the wheel rotating angular speed (expressed in rev/s).

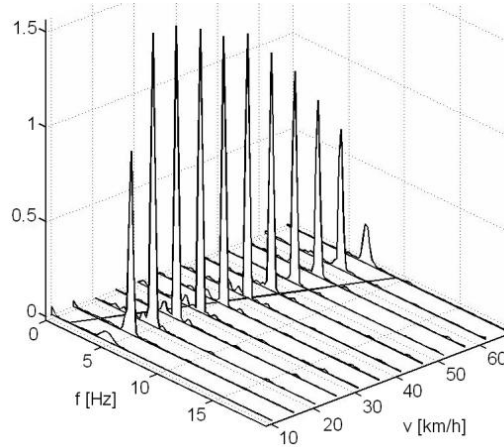


Figure 6 – FFT waterfall

($\varepsilon=34^\circ$; $N=40$ daN; Tire a; $p=1.2$ bar; $I_a=0.37\text{kgm}^2$; $I_w=0.324$ kgm^2 ; fork maximum extension; $\sigma=0.615\text{Nm/s/rad}$)

A basic survey was conducted to experimentally highlight the influence of some parameters on system dynamics. For each castor configuration, the system was perturbed by hitting one end of the handlebar and then observing if shimmy oscillation occurred. The test was repeated by increasing steering damping to detect the value for which the shimmy oscillation does not arise. The investigation results are reported as diagrams showing the damping required to stabilize the system versus the belt speed.

The experimental survey was conducted deducing the stability diagram for a castor “reference configuration” characterized by the following parameter values:

- rake, $\varepsilon=27^\circ$;
- tire pressure, $p= 1.2\text{bar}$;
- castor moment of inertia about the steering axis, $I_c = 0.37\text{kgm}^2$;
- wheel the moment of inertia, $I_w= 0.32$ kgm^2 ;
- castor weight, $W=40$ daN;
- additional vertical load, $N = 40$ daN;
- suspension extension, maximum;
- absence of rotational stiffness.

Since damper tuning is discrete, the damping threshold value is comprised between this curve and the one obtained considering the click immediately below (thin dashed curve in figure 7). In the following diagrams, only the upper curve will be considered.

Starting from the reference configuration and disassembling the steering damper, the castor results unstable in the range 10-70km/h and stable for speeds greater than 70km/h; during the

tests, the steering damper was not removed and so the lower damping value, reported in the stability diagrams, is 0.615Nsm/rad (click 0).

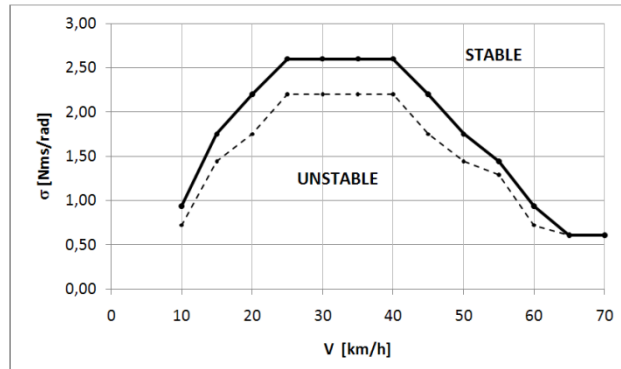


Figure 7 – **Stability diagram for reference configuration**
 ($\epsilon=27^\circ$; $N=40$ daN; Tire a; $p=1.2$ bar; $I_a=0.37\text{kgm}^2$; $I_w=0.32$ kgm^2 ; fork maximum extension)

The tests performed for this configuration (thick line in Figure 7) show that the necessary additional damping up to a certain speed value is minimum; as the belt velocity increases, a higher damping value is required to stabilize the system. When the speed is increased further, the necessary damping decreases up to a speed for which the minimum damping is required to stabilize the castor. For high speed values, the gyroscopic effect that arise due to fork lateral flexibility has a stabilizing effect on the system [3, 5].

The results of several tests, performed for different castor configurations, are reported in the figures below and compared with the reference configuration ones.

Figure 8 shows the influence of the vertical load; a comparison between the stability curve and the one obtained with an additional vertical load of 20daN is reported; the curve is located below the reference one and the increase in stability is due to a reduction in tire lateral force.

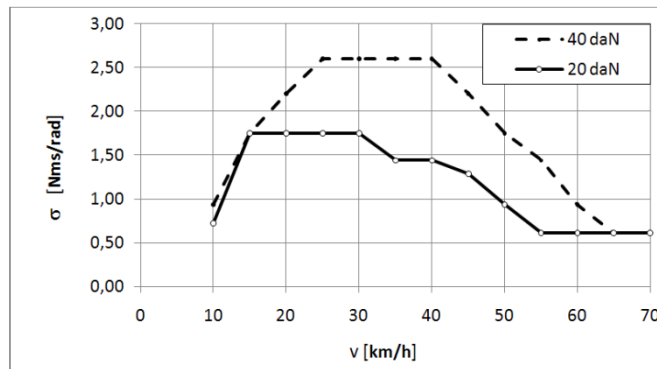


Figure 8 - **Vertical load influence**
 ($\epsilon=27^\circ$; $N=20$ daN; Tire a; $p=1.2$ bar; $I_a=0.37\text{kgm}^2$; $I_w=0.32$ kgm^2 ; fork maximum extension)

Improved stability and a reduction in the speed range, within which shimmy oscillations arise, is achieved by increasing lateral fork stiffness adopting the minimum fork extension configuration (figure 9) or increasing the rake angle from 27° to 34° (Figure 10). In this last configuration, a wider speed range for which the damping required to stabilize the system is constant was also observed.

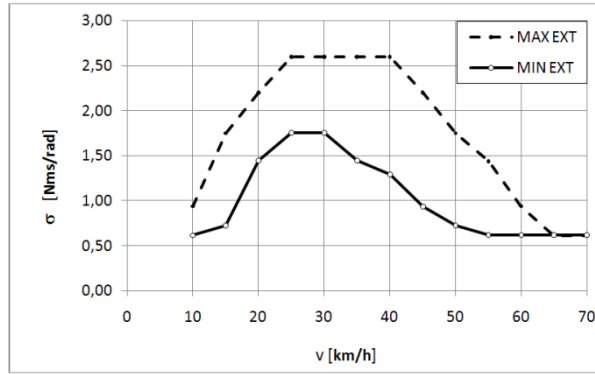


Figure 9 - **Suspension extension influence**
 ($\epsilon=27^\circ$; $N=40$ daN; Tire a; $p=1.2$ bar; $I_a=0.37\text{kgm}^2$; $I_w=0.32$ kgm^2 ; fork minimum extension)

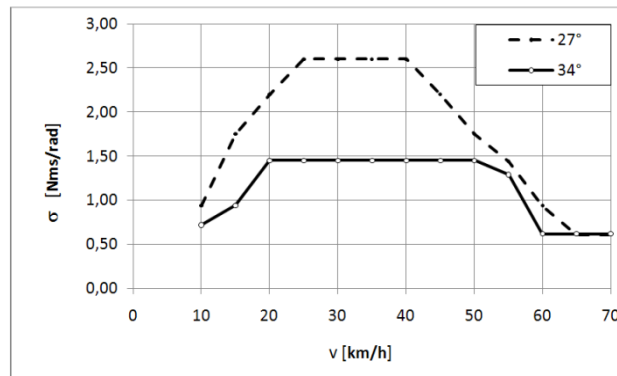


Figure 10 - **Castor angle influence ($\epsilon=34^\circ$)**
 ($\epsilon=34^\circ$; $N=40$ daN; Tire a; $p=1.2$ bar; $I_a=0.37\text{kgm}^2$; $I_w=0.32$ kgm^2 ; fork maximum extension)

Further improvement of stability is achieved by increasing rake angle and decreasing the vertical load as shown in Figure 11.

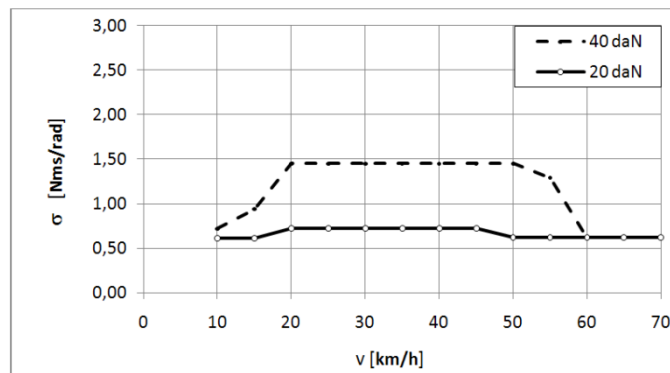


Figure 11 - **Vertical load influence for $\epsilon=34^\circ$**
 ($\epsilon=34^\circ$; $N=20$ e 40 daN; tire a; $p=1.2$ bar; $I_a=0.37\text{kgm}^2$; $I_w=0.32$ kgm^2 ; fork maximum extension)

- Greater stability with regard to shimmy is obtained by increasing the castor inertia properties:
- the diagram reported in Figure 13 refers to the addition of two 0.5kg masses at the ends of the handlebar, as shown in Figure 12 that implies an increment of the castor moment of inertia with respect to the steering axis from 0.37 kg/m^2 to 0.50 kg/m^2 (+35%) since the distance between the ends of the handlebar and the steering axis is 0.362m ;
 - the stability curve in Figure 15, on the other hand, was obtained by increasing the moment of inertia of the wheel with respect to the wheel axis using ten 60g balancing masses (Figure 14) fixed on the intrados of the wheel rim, at a distance of 0.18m from

the wheel axis resulting an increment of the wheel moment of inertia from 0.32 kg/m^2 to 0.34 kg/m^2 (+6.2%).

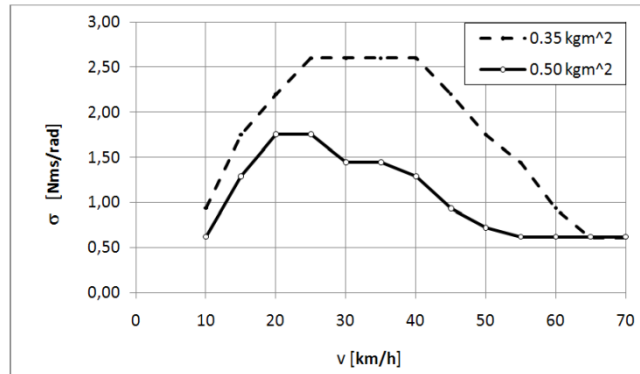
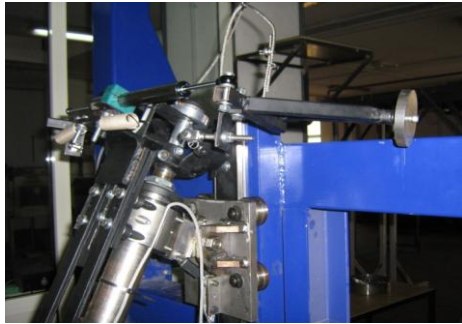


Figure 12, 13 – Masses on the handlebar ends; castor mass moment of inertia influence ($\epsilon=27^\circ$; $N=40 \text{ daN}$; tire a; $p=1.2 \text{ bar}$; $I_a=0.50 \text{ kgm}^2$; $I_w=0.32 \text{ kgm}^2$; fork maximum extension)

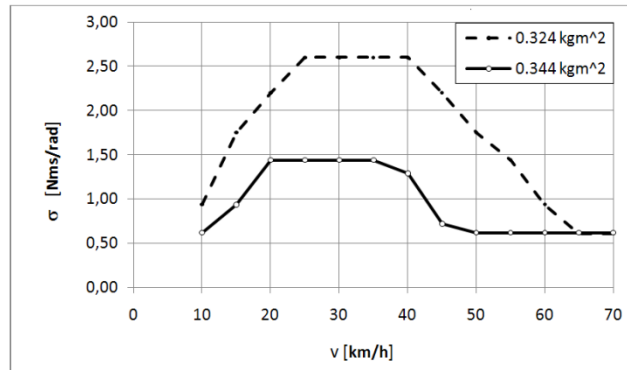


Figure 14, 15 –Additional masses on the rim; wheel mass moment of inertia influence ($\epsilon=27^\circ$; $N=40 \text{ daN}$; tire a; $p=1.2 \text{ bar}$; $I_a=0.37 \text{ kgm}^2$; $I_w=0.34 \text{ kgm}^2$; fork maximum extension)

Some tests were also conducted by taking rotational steering stiffness into account; two helical springs were connected to the castor providing a rotational stiffness of 0.14 Nm/rad ; we observed that, compared with the reference configuration, more damping is required to stabilize the castor. The diagram (Figure 16) shows the click adjustment versus the belt speed since a constant damping coefficient cannot be associated for more than 8 clicks.

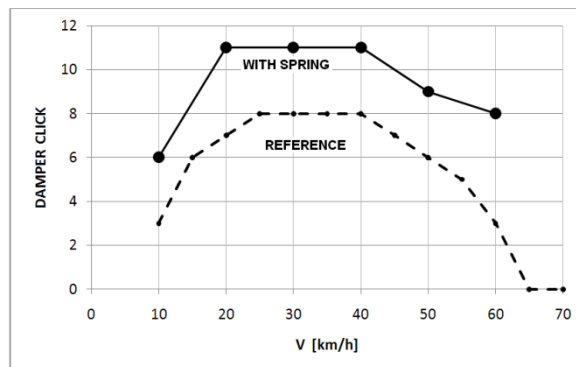


Figure 16 – Rotational stiffness influence ($\epsilon=27^\circ$; $N=40 \text{ daN}$; tire a; $p=1.2 \text{ bar}$; $I_a=0.37 \text{ kgm}^2$; $I_w=0.32 \text{ kgm}^2$; fork maximum extension; $k_\theta=0.14 \text{ Nm/rad}$)

4 CONCLUSIONS

A test rig for the experimental study of the shimmy phenomenon, with reference to the motorcycle front assembly, was developed in order to define the damping required to stabilize the castor. The paper includes several stability maps for different castor parameter values, reported in terms of damping-velocity diagrams. The investigation has mainly dealt with typical motorcycle parameter values.

In particular, since the vertical load and fork stiffness have opposite effects on the shimmy phenomenon, the castor installed on the belt rig was modified to avoid an increase in fork stiffness with the vertical load due to the shortening of the telescopic suspension; the investigation was conducted for the two extreme configurations, characterized by the maximum and the minimum extension of the fork respectively.

Acknowledgments

The authors are very grateful to Prof. V. Cossalter for encouraging the experimental work undertaken, supplying the tires used in the tests, already characterized at the University of Padua, and for his valuable discussions with the authors.

REFERENCES

- [1] W.J. Moreland, “The story of shimmy”, *Journal of Aeronautical Sciences* 21 (1954) 793–808.
- [2] H.B. Pacejka, “Analysis of the shimmy phenomenon”, *Proceedings of the Institute of Mechanical Engineers*, 1965.
- [3] R.S. Sharp, “The stability and control of motorcycles”, *Journal of Mechanical Engineering Science* 13 (5) (1971).
- [4] V. Cossalter, *Motorcycle Dynamics*, Lulu Editor 2006, ISBN 978-1-4303-0861-4.
- [5] D. De Falco, G. Di Massa, S. Pagano, “On castor dynamic behavior”, *Journal of the Franklin Institute* n.347 , (2010), pp. 116–129.
- [6] D. De Falco, G. Di Massa, S. Pagano – “A methodology for characterization of motorcycle out of plane natural modes” - *CM2009, The Sixth International Conference on Condition Monitoring and Machinery Failure Prevention Technologies* - Dublin, Ireland, 23 – 25 June, 2009.